AD-A080 491   MASSACHUSETTS INST OF TECH LEXINGTON LINCOLN LAB   F/6 9/5
               CHARACTERIZATION OF TRANSCONDUCTANCE MULTIPLIER WEIGHT CIRCUITS--ETC(U)
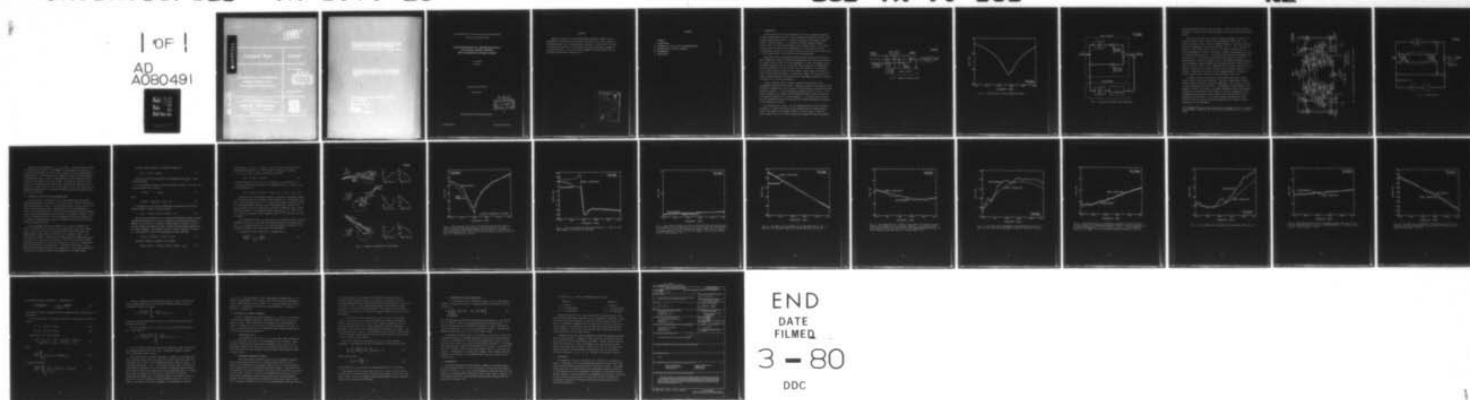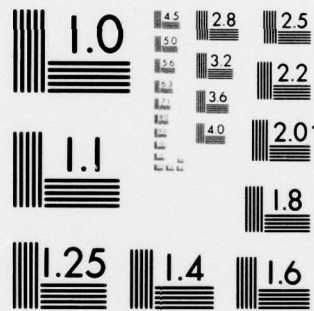   JUN 79   B C LEVENS   F19628-78-C-0002
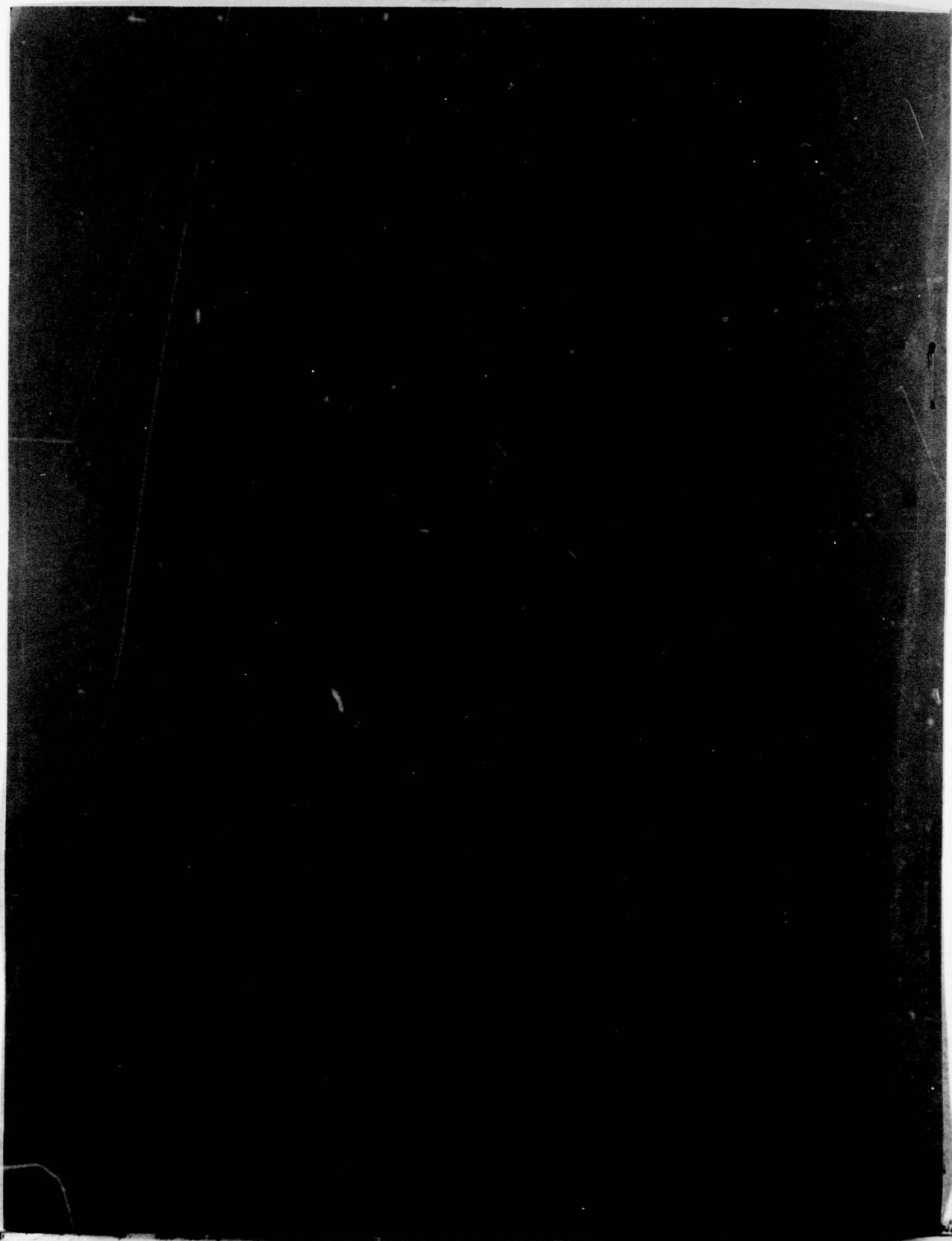UNCLASSIFIED   TN-1979-23   ESD-TR-79-161   NL

| OF |
AD
A080491

END
DATE
FILMED
3-80
DDC

MICROCOPY RESOLUTION TEST CHART
NATIONAL BUREAU OF STANDARDS-1963-A

MASSACHUSETTS INSTITUTE OF TECHNOLOGY

LINCOLN LABORATORY

CHARACTERIZATION OF TRANSCONDUCTANCE
MULTIPLIER WEIGHT CIRCUITS
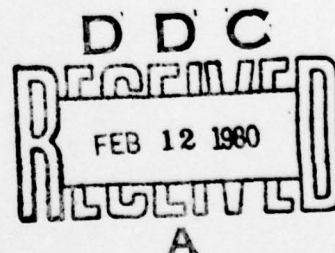# FOR AN ADAPTIVE ANTENNA SYSTEM

B. C. LEVENS

Group 68

TECHNICAL NOTE 1979-23

22 JUNE 1979

DDC

FEB 12 1980

A

LEXINGTON   MASSACHUSETTS

ABSTRACT

Extensive testing of the transconductance multiplier weight circuits designed for the antenna nulling project indicates that a simple time delay feedthrough model fits the measured data very well. Properties of this model are derived and applied to the problem of determining the model parameters from measured data. Plots of actual measurements and model predictions are provided to demonstrate goodness of fit.

CONTENTS

I.   INTRODUCTION

Recently, there has been much interest in the use of Adaptive Antennas
in Space Communications systems. These antennas are expected to cancel inter-
ference signals automatically. The basic structure of an Adaptive Antenna
system is shown in Figure 1. It consists of several antenna elements, a
weight circuit for each antenna element, and a control circuit. The control
circuit senses the direction and magnitude of the interference and sets
the amplitude and phase of the weight circuits in such a way as to form a null
in the antenna pattern in the direction of the interference.

Experience with an experimental Adaptive Antenna system has shown that
when attempting to obtain interference cancellation over a non-zero bandwidth
the weight circuits often limit the performance. In fact, the weight circuit
performance appears to be one of the most critical features in determining
how much cancellation can be obtained. For this reason, it is desirable to
have a simple analytical model for the weight circuits which can be used to
predict cancellation performance. Having such a model, one could specify in
terms of model parameters the weight circuit requirements necessary to achieve
a desired level of system performance.

Several different types of weight circuits were evaluated in the
experimental Adaptive Antenna system. Though they differ in configuration and
performance significantly, the circuits all have roughly the same characteristic
frequency response.   A typical frequency response is shown in Fig. 2. This
figure represents the response obtained when the weight circuit is adjusted
for maximum attenuation at a single frequency. It is clear from the figure
that the acheivable attenuation averaged over a band of frequencies decreases
as the bandwidth increases.

The resemblance of Figure 2 to such familiar patterns as the frequency
response of a single-zero digital filter suggests that the simple model of
Figure 3 may apply for the weight circuits. In this figure we model the
actual weight circuit as an ideal weight with an additive term of unweighted,

1
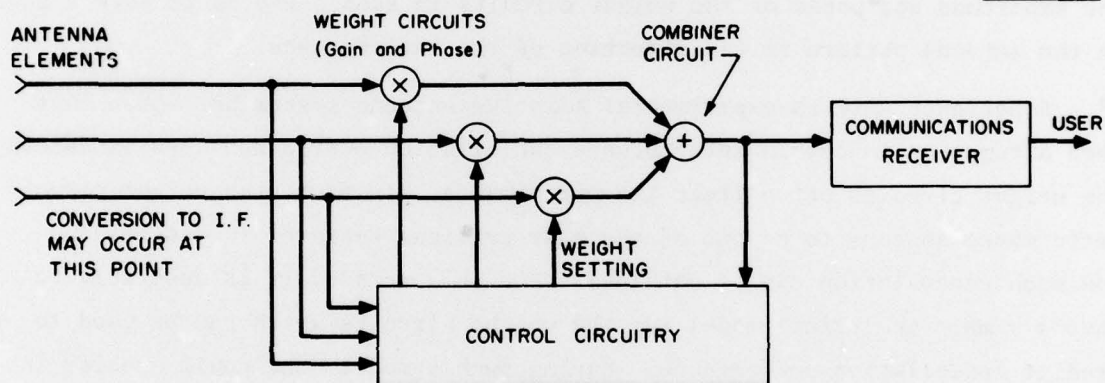
Fig. 1. Adaptive antenna system.
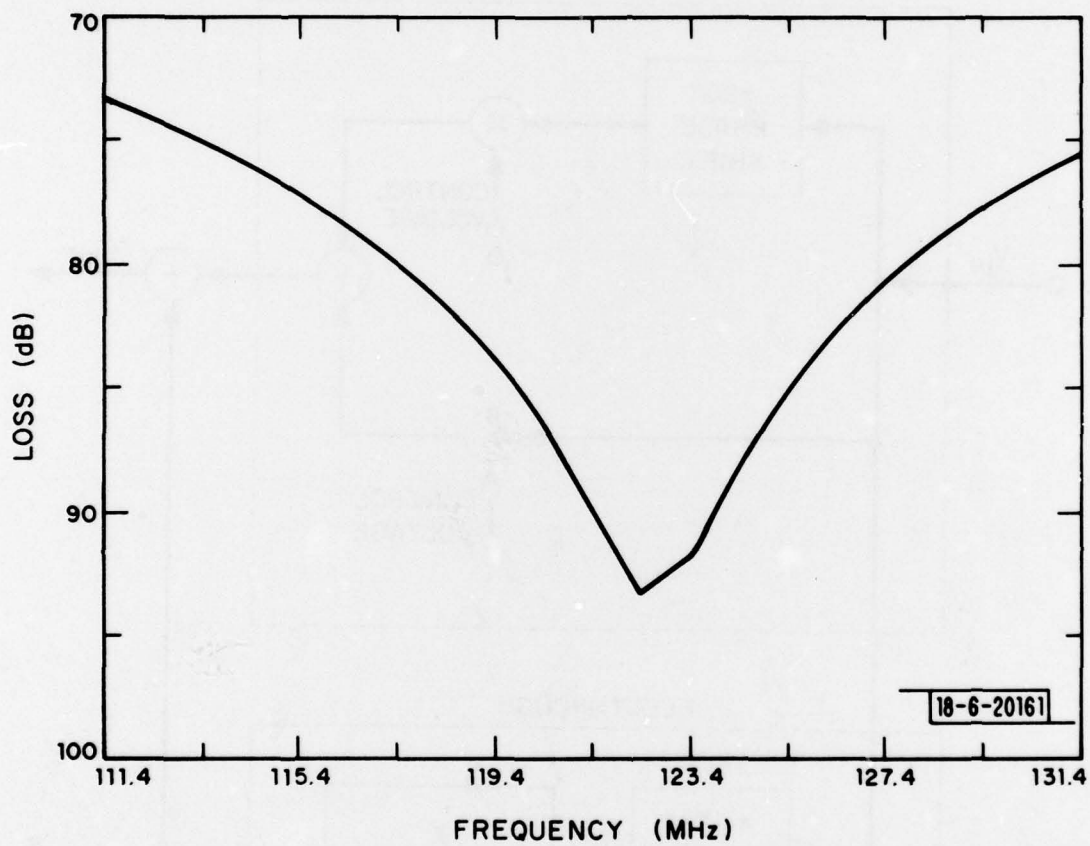
Fig. 2. Typical weight circuit frequency response.

3

IDEAL WEIGHT

$-90°$ PHASE SHIFT

CONTROL VOLTAGE Q

V_{IN}

$\times$

$+$

$+$

V_{OUT}

$\times$

CONTROL VOLTAGE I

FEEDTHROUGH

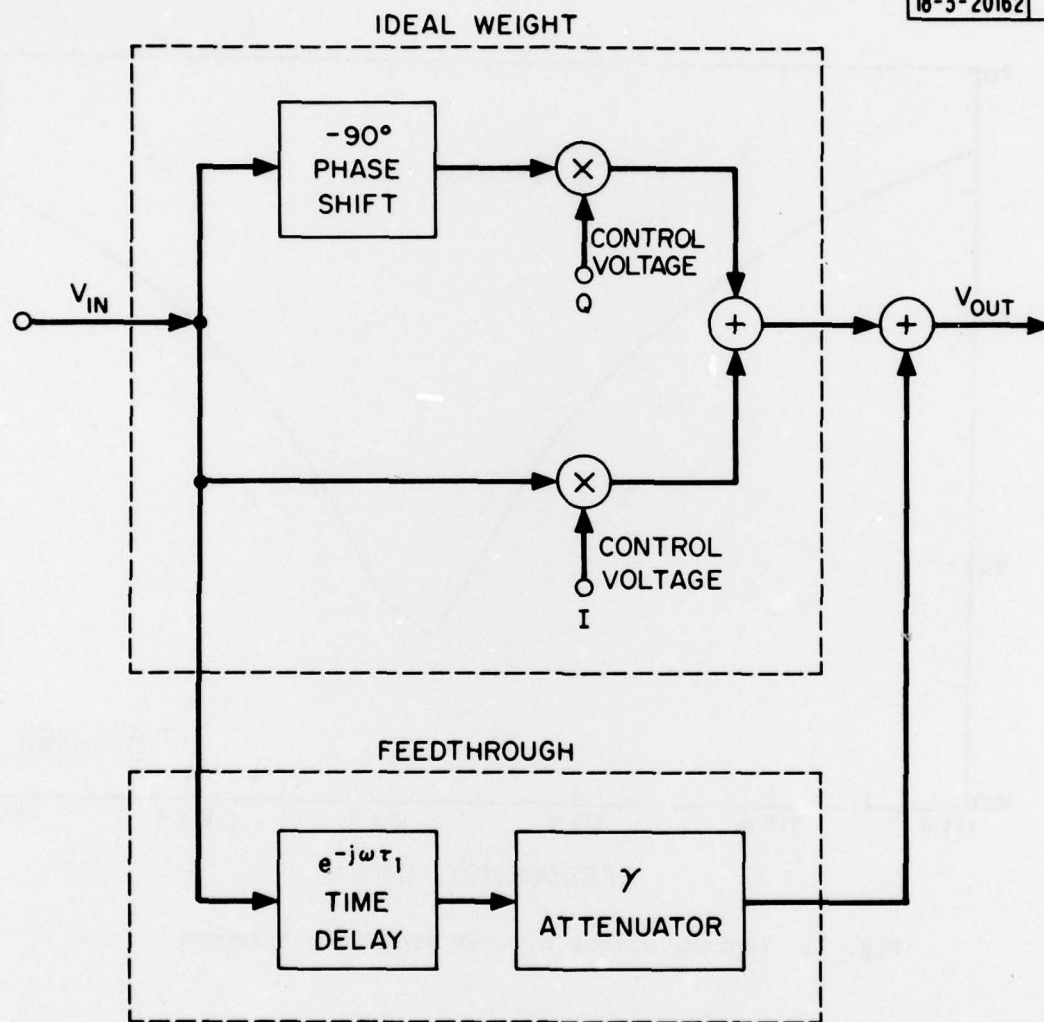$e^{-j\omega\tau_1}$ TIME DELAY

γ ATTENUATOR

Fig. 3. Weight circuit model with feedthrough.

4

but delayed feedthrough from input to output. Despite this model's apparent simplicity it has been found to be applicable to a variety of different weight circuits.

This report addresses the problem of fitting the model of Figure 3 to a particular weight circuit design--the transconductance multiplier. The general structure of this circuit is shown in Figure 4. Note that the weight setting is determined by two control voltages V_I and V_Q. For a complete description of this circuit see TN 1979-11[*]. In order to confirm that time delayed feedthrough is indeed a valid model, extensive measurements were made on individual weight circuits. Calculations were then made to determine what values of γ and τ (from Figure 3) give the best overall fit of model to measurement for a particular weight circuit. The measured frequency response and the frequency response predicted by the model were then plotted on the same set of axes so that a visual comparison could be made. These plots were made for a wide variety of weight settings over a frequency range of 121.4 ±10 MHz. Inspection of the plots (see for example Figures 7 through 16) reveals that the model predicts the observed behavior very well.

It should be borne in mind that a more complete model must include several effects other than feedthrough. These are illustrated in Figure 5. Several features of Figure 5 should be emphasized. First, there is an over-all delay associated with the device. The mismatch of this parameter from channel to channel (see Figure 1) is another potential source of performance degradation in the antenna system; however, it is not as important as the feedthrough because measures can be taken to trim out variations in this parameter (see TN 1979-11). The over-all delay is mentioned here only because it must be subtracted from the measured data in order to obtain a measurement of the feedthrough.

---

[*]J. N. Wright, "Transconductance Multipliers for Weight Circuits in an Adaptive Nulling System," Technical Note 1979-11, Lincoln Laboratory, M.I.T. (1 June 1979)
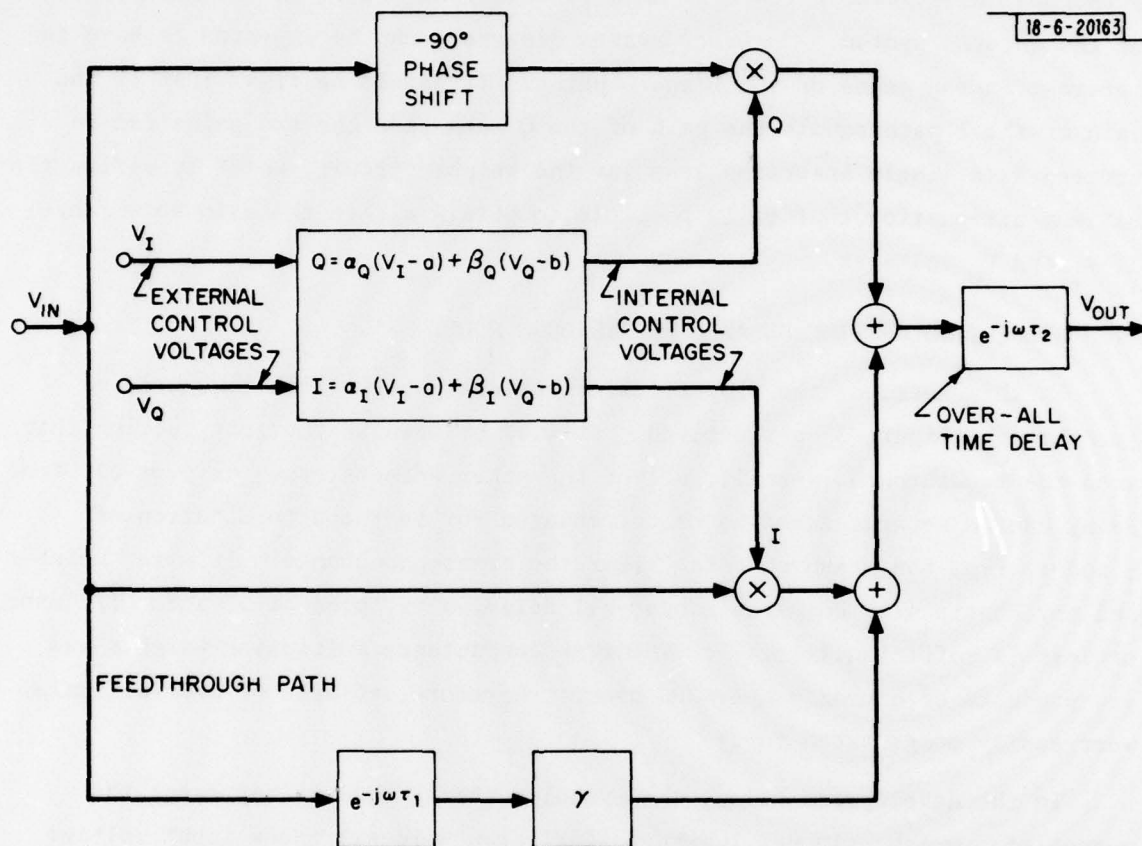
Fig. 4. Transconductance multiplier weight circuit schematic.

6
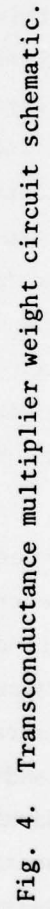
Fig. 5. Complete model.

Second, are the parameters α_I, α_Q, β_I, and β_Q. These have been included to indicate that the gains of the inphase (I) and quadrature (Q) paths are not precisely equal and that the V_I and V_Q voltages do not represent perfectly orthogonal axes. These features have virtually no effect on the performance of the antenna system. However, system designers can be expected to have an interest in the gains of the I and Q paths. It should be clear that if the gain of the I path equals the gain of the Q path then the two gains can be treated as a single insertion loss for the weight circuit, which specifies the minimum attenuation that it is possible to obtain within the allowable range of V_I and V_Q voltages.

II. PROPERTIES OF TIME DELAYED FEEDTHROUGH MODEL

In this section, the properties of an ideal weight with time delayed feedthrough (Figure 3) are derived. It will be seen in the next section that when the feedthrough is small, all of the other effects, such as over-all time delay can be separated and hence compensated for in the determination of γ and τ_1 from the measured data. (For the transconductance multiplier weights and any others with comparable over-all delay, a $\gamma\tau_1$ product of about 1/2 nsec. or less is sufficiently small. The transconductance multiplier weights had $\gamma\tau_1$ products of approximately 250 psec.; therefore, effects of over-all delay were easily compensated for.)

In the development below, the symbol $V_o(t)$ is used to represent the output of a weight circuit (whether ideal or non-ideal) whose input voltage $V_{in}(t) = \cos\omega t$. Since both the ideal multiplier and the multiplier with feedthrough are linear devices as far as V_{in} is concerned, (that is, for fixed control voltage) it should be clear that scaling the input signal $V_{in}(t)$ by a factor of K also scales the output by a factor of K, and that shifting the phase of the input (for example, using $V_{in}(t) = \cos(\omega t + \phi)$) shifts the phase of the output by the same amount. A closely related symbol is $|V_o|$, which denotes the peak amplitude of the signal $V_o(t)$. With these definitions in mind, we can proceed to develop the properties of the weight model.

8

An ideal weight (Figure 3) is defined by Equation 1:

$$V_o(t) = I\cos\omega t + Q\sin\omega t \tag{1}$$

where $V_o(t)$ has been normalized by the assumption that $V_{in}(t) = \cos\omega t$ as described above.

It is clear that in order to obtain an output of $A\cos(\omega t + \phi)$, the I and Q control voltages must be set to

$$I = A\cos\phi \qquad Q = -A\sin\phi \tag{2}$$

since

$$\cos\phi\cos\omega t - \sin\phi\sin\omega t = \cos(\omega t + \phi) \tag{3}$$

Incorporating a time delayed feedthrough in parallel with the ideal weight as shown in Figure 3 yields equation 4.

$$V_o(t) = I\cos\omega t + Q\sin\omega t + \gamma\cos(\omega t - \omega\tau_1) \tag{4}$$

We have now unfortunately lost the simple relationship between the output amplitude and phase and the control voltage that is expressed by equation 2, however, we can recover it by making a simple change of variables. We can set the in-phase and quadrature terms to cancel the feedthrough completely at any single frequency. The equation we have to solve is equation 5 in which ω_o is the frequency at which the feedthrough is being cancelled.

$$I_c\cos\omega_o t + Q_o\sin\omega_o t = -\gamma\cos(\omega_o t - \omega_o\tau_1) \tag{5}$$

Using the identity of equation 3, we obtain:

$$(\cos\omega_o\tau_1)\cos\omega_o t - (\sin\omega_o\tau_1)\sin\omega_o t = \cos(\omega_o t - \omega_o\tau_1) \tag{6}$$

9

hence setting $I_o = -\gamma\cos \omega_o\tau_1$ and $Q_o = -\gamma\sin \omega_o\tau_1$ will completely null the feedthrough at frequency ω_o. If we now make the change of variables $I = I_o + I_x$, $Q = Q_o + Q_x$ then at frequency ω_o we have:

$$V_o(t) = I_x\cos\omega_o t + Q_x\sin\omega_o t \qquad (7)$$

To obtain an output of $A\cos(\omega_o t + \phi)$ at frequency ω_o, we need only set I_x and Q_x as indicated by equation 2. An expression for $V_o(t)$ that is valid at all frequencies is:

$$V_o(t) = I_x\cos\omega t + Q_x\sin\omega t + (\cos(\omega t - \omega\tau_1) - \cos(\omega t - \omega_o\tau_1)) \quad (8)$$

Insight into the feedthrough model may be obtained by considering Figure 6. This Figure shows that equation 4 may be pictured as a fixed phasor $(I - jQ)$ plus a small rotating phasor $\gamma e^{-j\omega\tau}1$. Study of the figure for various values of I and Q should make clear why some of the measured data (Figures 7-16) shows curvature in only the phase plot, some only in amplitude, some in both, and some in neither. The assumption made in drawing Fig. 6 is that ω varies over a range of frequencies small enough so that $\gamma e^{-j\omega\tau}1$ sweeps out less than 1/2 radian.

Let us suppose now that ω_o is the center of the frequency band of interest Although it will not be clear until the next section why we are interested in this, let us compute the slope at ω_o of both the amplitude and phase of the frequency response of the ideal weight with feedthrough.

The amplitude slope in dB/rad/sec is proportional to:

$$\frac{\partial\ln|V_o|^2}{\partial\omega} = \frac{1}{|V_o|^2} \frac{\partial|V_o|^2}{\partial\omega} \qquad (9)$$
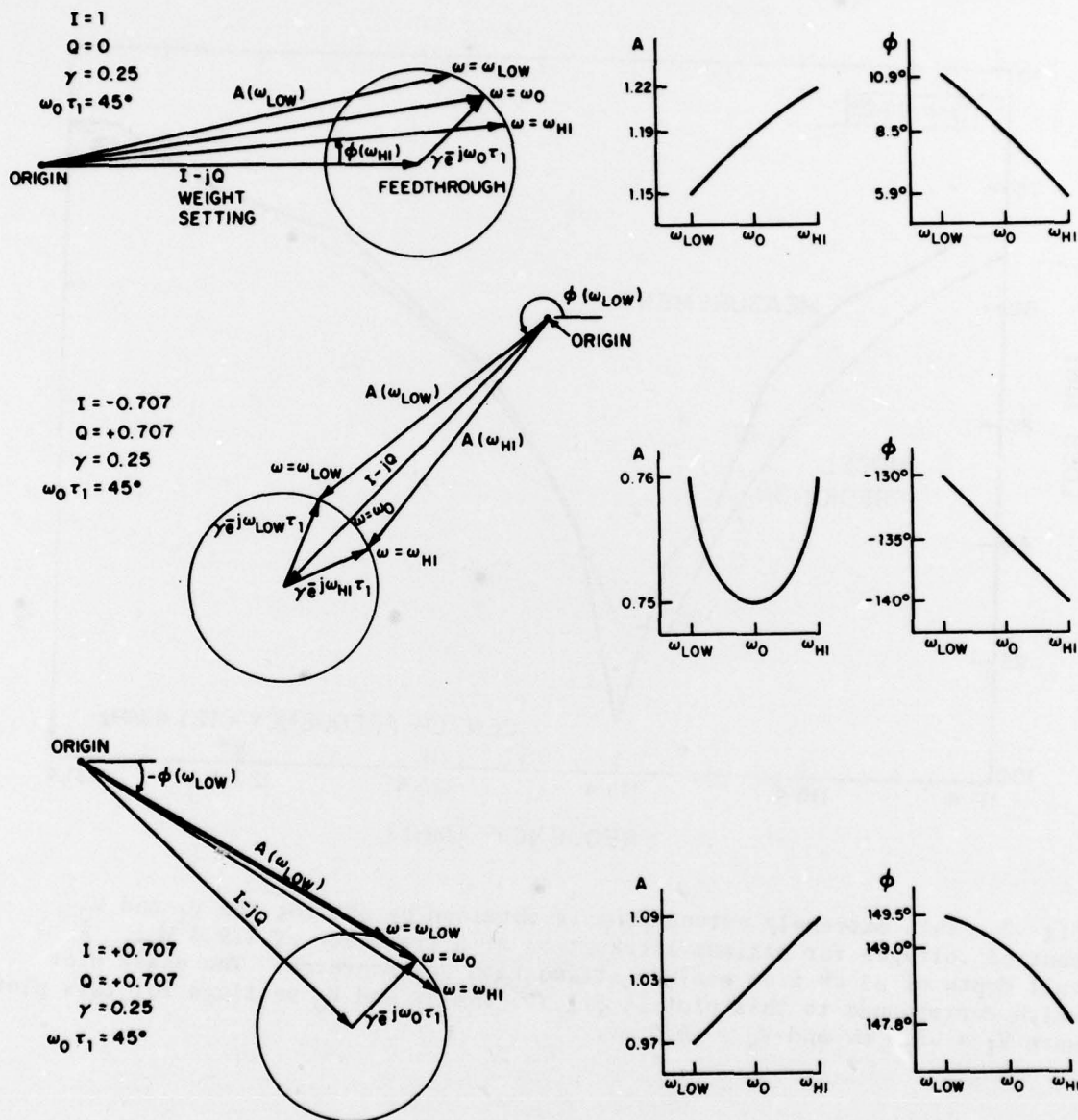
10

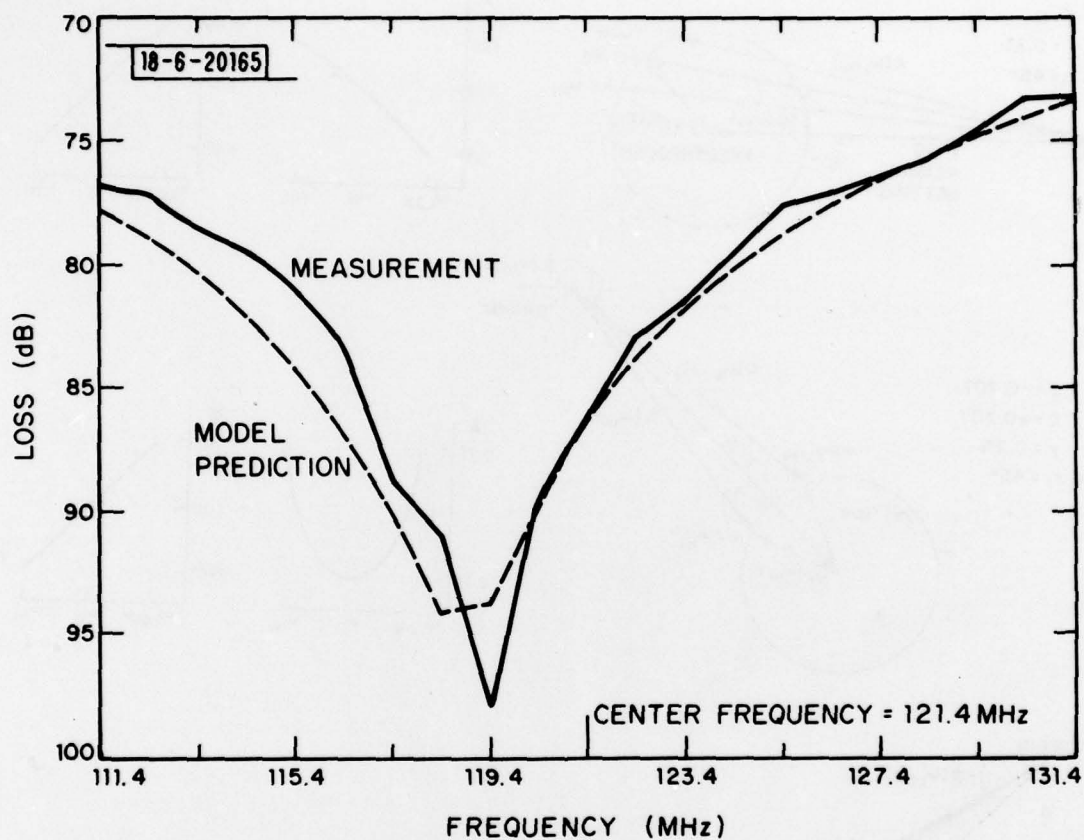Fig. 6. Graphical illustration of feedthrough.

Fig. 7. This extremely curved plot is obtained by setting the V_I and V_Q control voltages for maximum attenuation at a frequency of 119.4 MHz. A null depth of 85 dB from minimum attenuation was achieved. The phase plot which corresponds to this plot is Fig. 8. The V_I and V_Q settings for this plot were V_I = -5.0 mv and V_Q = -6.0 mv.
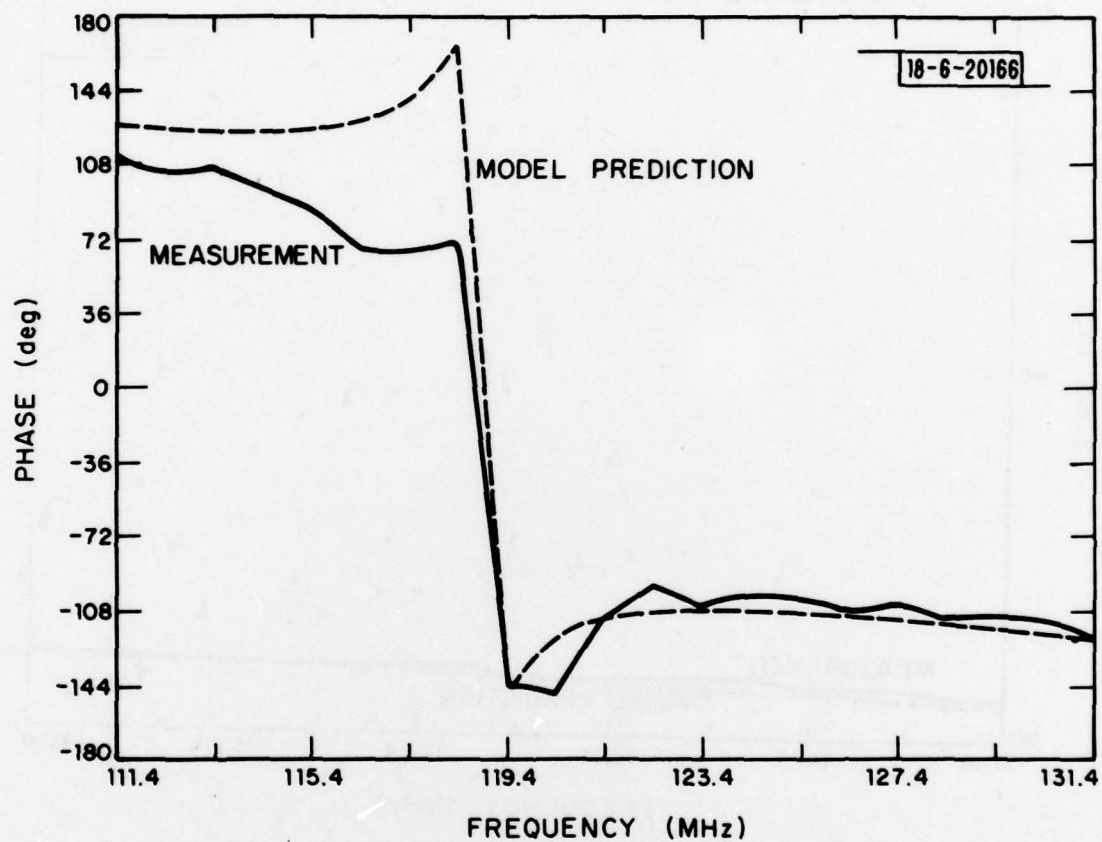
12

Fig. 8. This is the phase plot which goes with Fig. 7. Note the large phase change in the vicinity of the null.
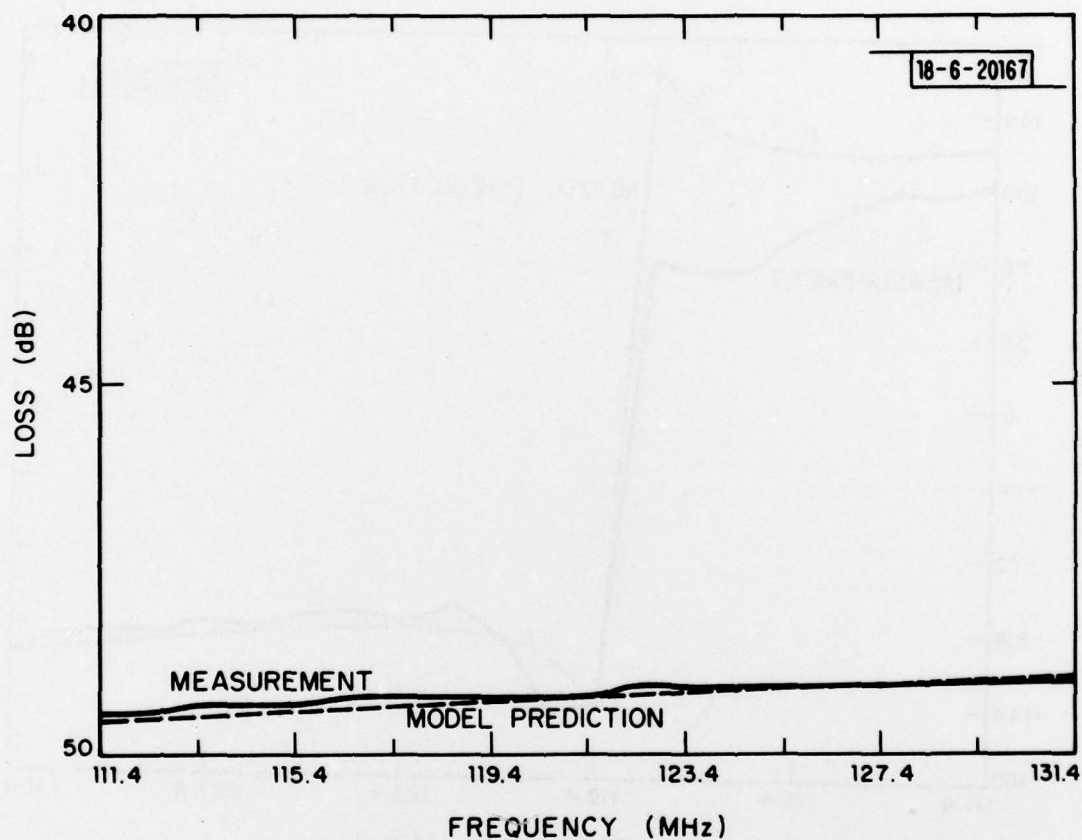
13

Fig. 9. This almost straight-line plot is obtained by setting V_I and V_Q for an attenuation at center frequency at 49.20 dB and a phase at center frequency of -47.2°. This plot would be suitable for curve fitting since it and its corresponding phase plot (Fig. 10) are so straight. The V_I and V_Q settings were V_I = 10 mv and V_Q = 0.0 v.

14
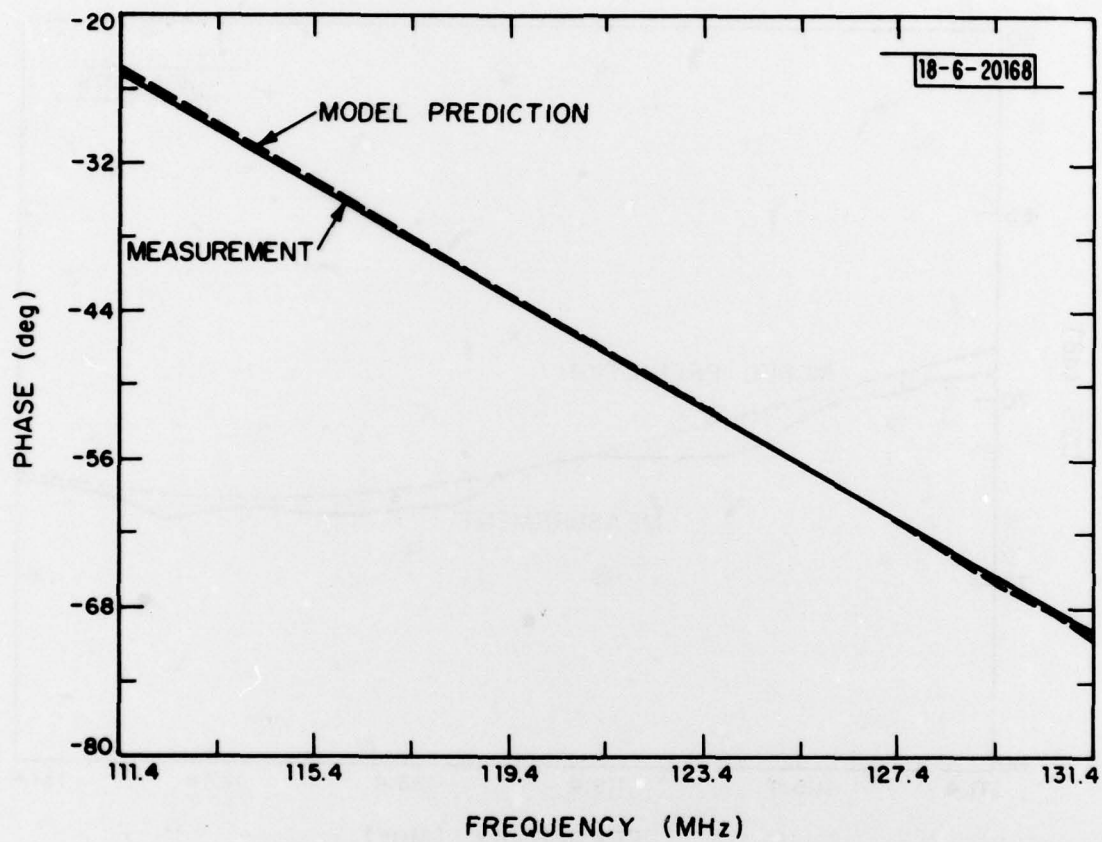
Fig. 10. This phase plot corresponds to the amplitude plot of Fig. 9.
Nearly all of the phase slope here is due to the overall delay (τ_2).

15
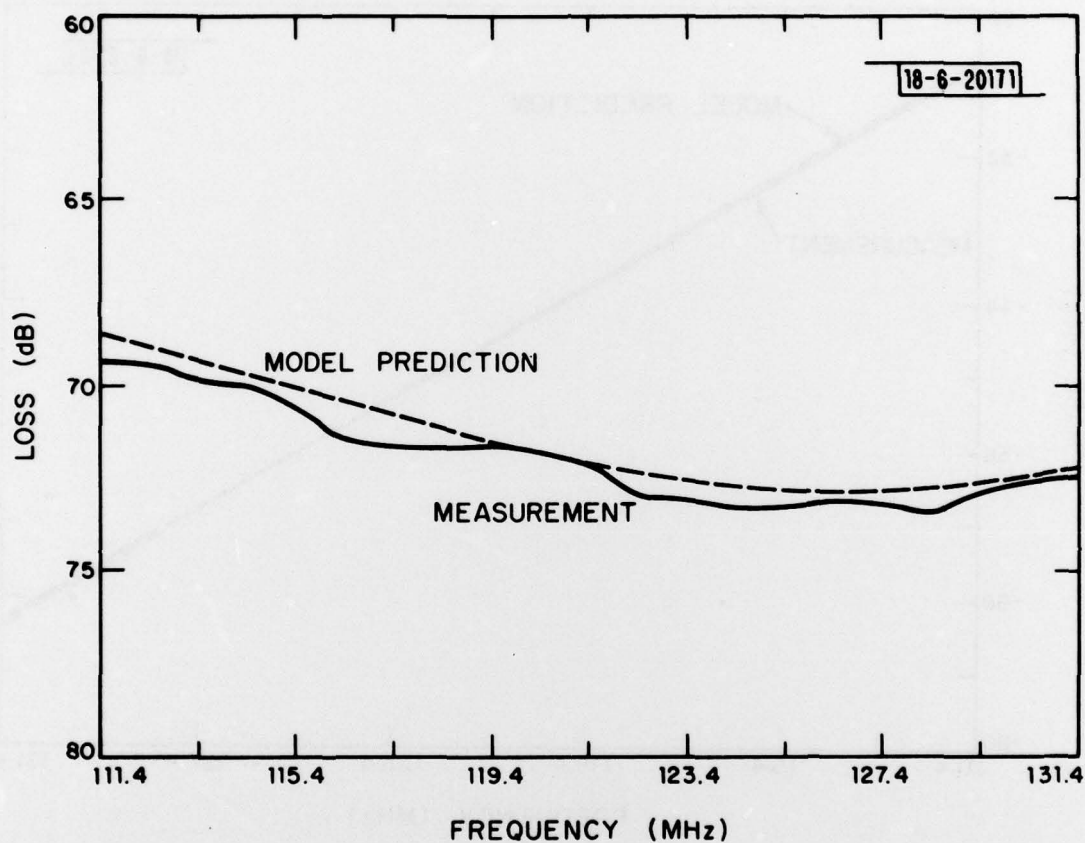
Fig. 11. This amplitude plot exhibits a fair amount of curvature and hence would not be suitable for curve fitting. However, it illustrates the predictive powers of the model nicely as does its companion phase plot (Fig. 12). The V_I and V_Q settings here were V_I = -6 mv and V_Q = -6 mv.
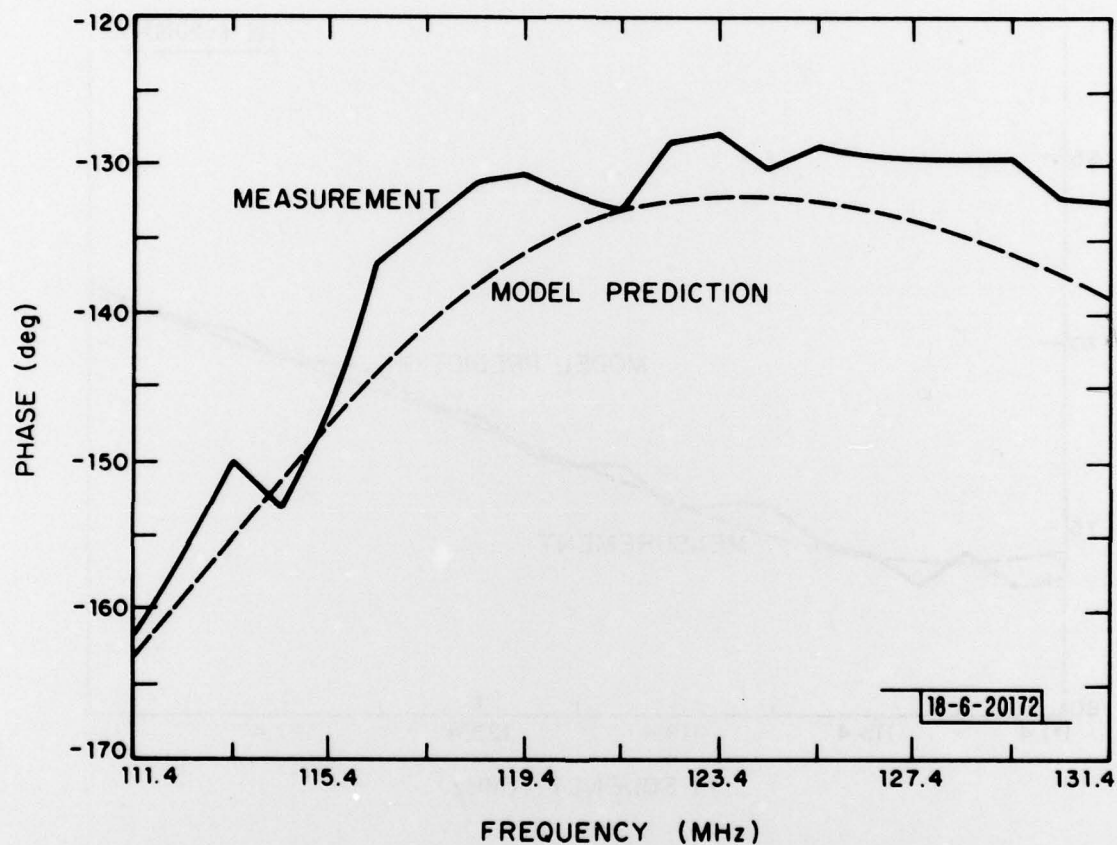
Fig. 12. This phase plot corresponds to the amplitude plot of Fig. 11.
Note how noisy the phase measurement is when the attenuation is great.

17
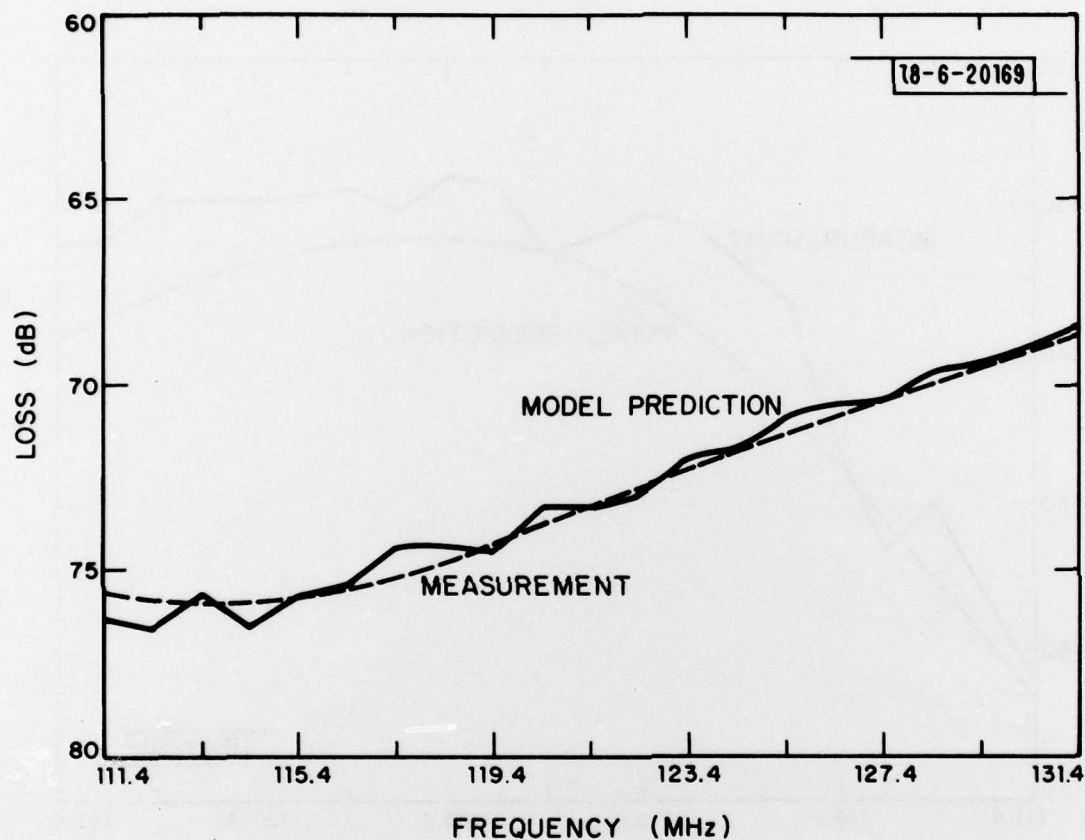
Fig. 13. This amplitude plot is sufficiently straight to be used for curve fitting, however, its corresponding phase plot (Fig. 14) is not straight at all. The control voltages are V_I = -5.0 mv and V_Q = -5.0 mv. Note how much difference a 1 mv change in V_I and V_Q can make (compare with Figs. 11 and 12).
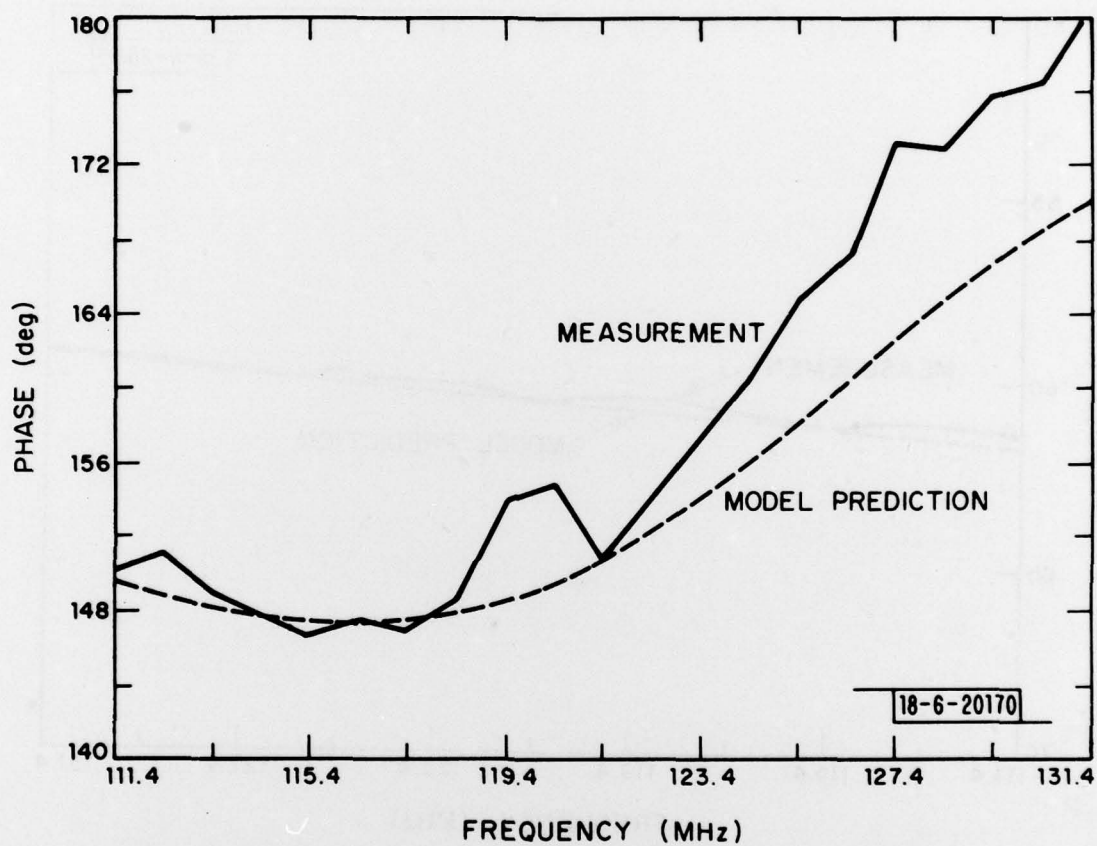
Fig. 14. This phase plot corresponds to the amplitude plot of Fig. 13.

18-6-20173

Fig. 15. This amplitude plot and its corresponding phase plot (Fig. 16) are straight enough to be used in the curve fitting procedure. The control voltages were V_I = -5.0 mv and V_Q = -1.0 mv.

20
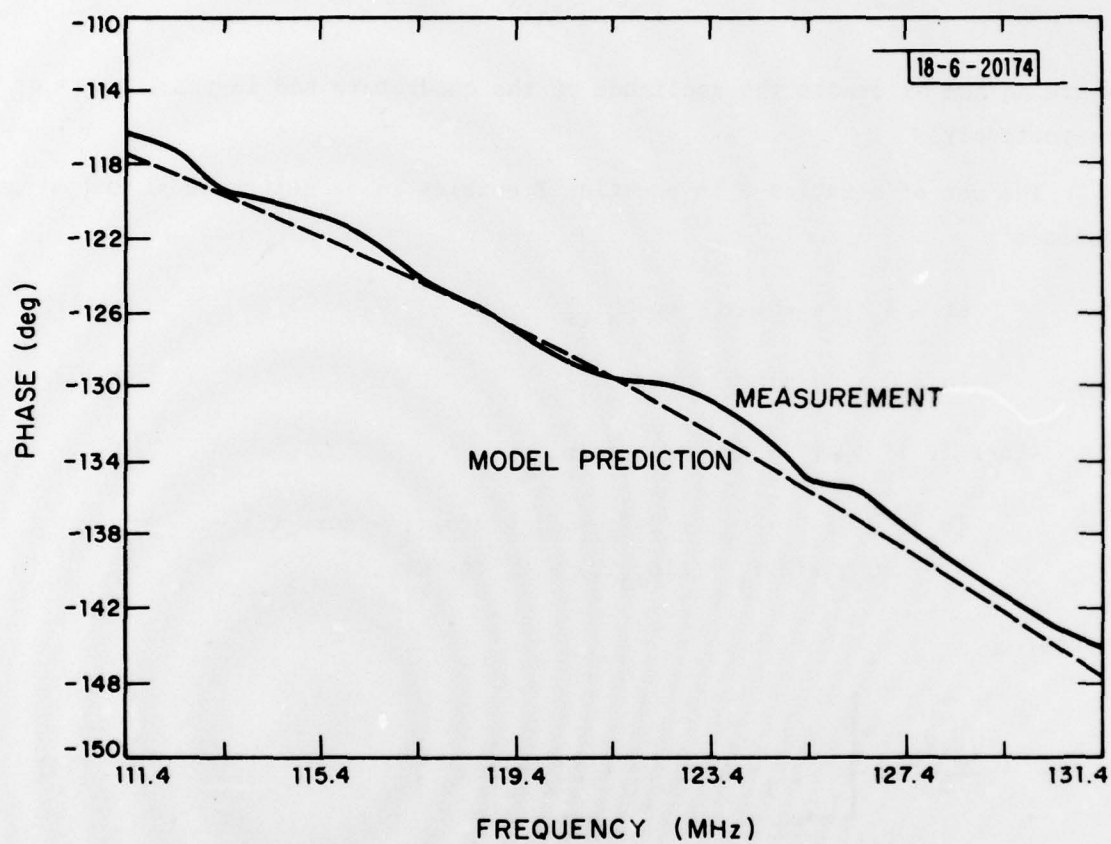
Fig. 16. This phase plot corresponds to the amplitude plot of Fig. 15.
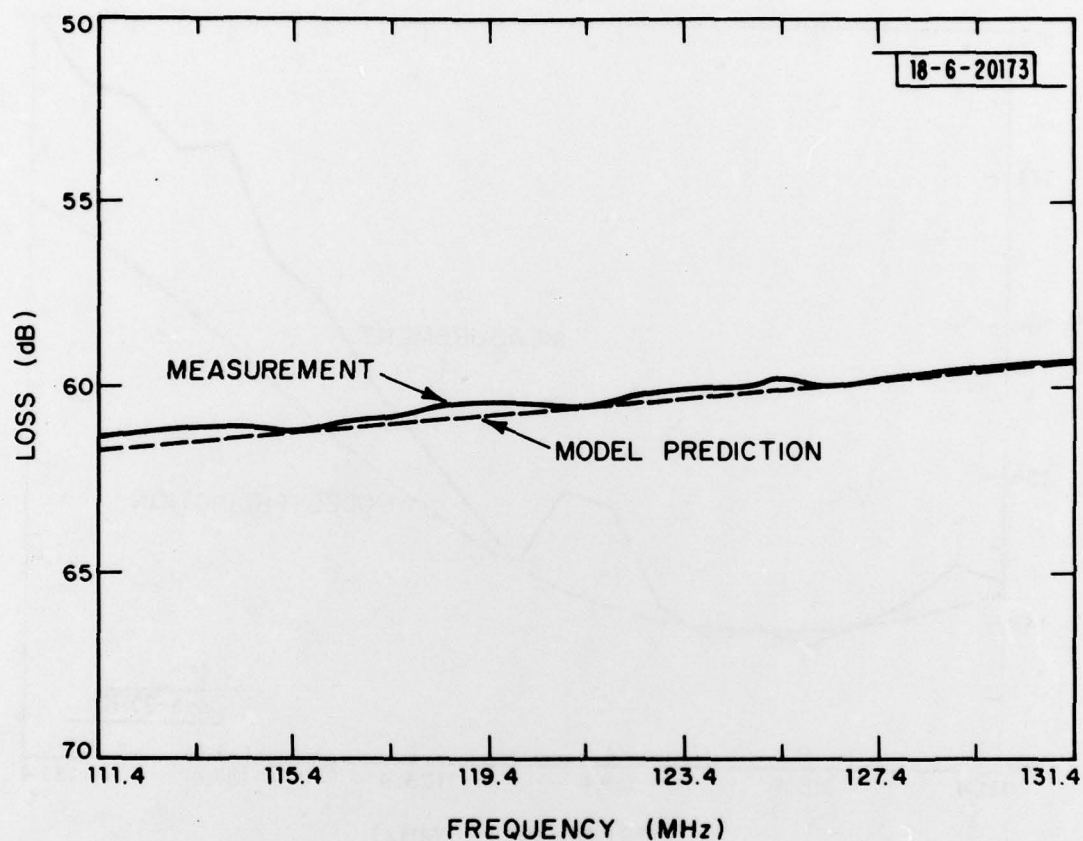Note that this phase measurement is less noisy than those made at greater
attenuation (See Figs. 12 and 14).

and the phase slope in deg/rad/sec is proportional to

$$\frac{-\partial\tan^{-1}(Aq/Ai)}{\partial\omega} = \frac{-1}{1 + Aq^2/Ai^2}\frac{\partial(Aq/Ai)}{\partial\omega} \tag{10}$$

where Aq and Ai denote the amplitude of the quadrature and in-phase parts of V_o respectively.

The use of equation 3 in equation 8 enables us to determine Ai and Aq as follows:

$$Ai = I_x + \gamma(\cos\omega\tau_1 - \cos\omega_o\tau_1) \tag{11}$$

$$Aq = Q_x + \gamma(\sin\omega\tau_1 - \sin\omega_o\tau_1) \tag{12}$$

Since $|V_o|^2 = Ai^2 + Aq^2$ we obtain:

$$|V_o|^2 = (I_x^2 + Q_x^2 + 2\gamma^2) + 2I_x\gamma(\cos\omega\tau_1 - \cos\omega_o\tau_1) + 2Q_x\gamma(\sin\omega\tau_1 - \sin\omega_o\tau_1) - 2\gamma^2\cos(\omega\tau_1 - \omega_o\tau_1) \tag{13}$$

Hence:

$$\frac{\partial|V_o|^2}{\partial\omega}\Bigg|_{\omega=\omega_o} = -2I_x\gamma\tau\sin\omega_o\tau_1 + 2Q_x\gamma\tau\cos\omega_o\tau_1 \tag{14}$$

By equation 9 we have:

$$\frac{\partial\ln|V_o|^2}{\partial\omega}\Bigg|_{\omega=\omega_o} = \frac{2\gamma\tau}{I_x^2 + Q_x^2}(Q_x\cos\omega_o\tau_1 - I_x\sin\omega_o\tau_1) \tag{15}$$

22

Finally, by making the substitution of equation 2 (where A denotes the center frequency amplitude and ϕ the center frequency phase) and using a trigonometric identity we obtain:

$$S_a = \frac{K_a}{2} \left. \frac{\partial \ln|V_o|^2}{\partial \omega} \right|_{\omega=\omega_o} = \frac{-K_a \gamma \tau_1}{A} \sin(\omega_o \tau_1 + \phi) \tag{16}$$

where S_a denotes the amplitude slope and K_a is a positive constant which is dependent on the units.

By means of equations 10, 11, and 12, we can obtain the phase slope as well. The result is:

$$S_p = \left. \frac{-K_p \partial \tan^{-1}(Aq/Ai)}{\partial \omega} \right|_{\omega=\omega_o} = \frac{-K_p \gamma \tau_1}{A} \cos(\omega_o \tau_1 + \phi) \tag{17}$$

It will be seen in the next section that equations 16 and 17 are useful in obtaining numerical values for γ and τ_1 from swept frequency response data on individual weight circuits.

One issue needs to be briefly discussed. In equation 4 the feedthrough term is shown as being a pure time delay of the input without any additional fixed phase shift. That is, the feedthrough term was shown as $\gamma \cos(\omega t - \omega \tau_1)$ rather than say $\gamma \sin(\omega t - \omega \tau_1)$. It turns out, however, that on the basis of a narrow-band measurement, it is not possible to distinguish between models which differ by only a fixed phase shift in the feedthrough path. For example, if one were to attempt to fit the data to a model with a sinusoidal feedthrough term rather than a cosinusoidal term one would obtain equally as good a fit. The only difference would be different values for γ and τ_1; however, the product $\gamma \tau_1$ would be unchanged. By narrowband we mean that

23

$\tau_1(\Delta\omega) < 1/2$. The measurements of the transconductance weights had a $\tau_1(\Delta\omega)$ product of approximately 1/4; therefore, they were narrow band measurements and the above ambiguity applies to them. It is known, however, that only the product $\gamma\tau_1$ is important in specifying system performance; therefore, the ambiguity is unimportant.

III. DETERMINATION OF MODEL PARAMETERS

In order to determine the model parameters γ, τ_1, and τ_2 it is necessary to measure the frequency response of the weight circuits for a variety of weight settings. These measurements can be made with a network analyzer. Figures 7 through 16 are typical plots of the data measured in this way. As done in the previous section, let us denote the center frequency amplitude by A and the center frequency phase by ϕ.

A.   Determination of τ_2

From equation 17 we see that if A is made large enough (compared to $\gamma\tau_1$) then the phase slope due to the feedthrough will be very small. Hence any phase slope which does appear when the weight circuit is set for low attenuation (large A) will be due only to the overall time delay, τ_2. This phase slope must first be subtracted from all measured phase slopes in order to obtain γ and τ_1.

B.   Solution of Equations 16 and 17

The network analyzer should be used to obtain frequency response data with the control voltages set to obtain several values of A and ϕ. Values of A corresponding to attenuations from -45 dB to -70 dB were found to be most useful for the transconductance multiplier weights. These values for A correspond to the actual attenuation of the device--no correction for average insertion loss is implied. Out of all the measured data some cases will be found to have amplitude and phase characteristics which are approximately straight over the frequency band of interest (see for example Figures 9 and 10). To minimize the effects of noise on slope determination these are the only

24

cases which should be considered in the solution of Equations 16 and 17. One should take enough measurements to be able to pick about 8 cases with straight amplitude and phase characteristics and a good spread of ϕ values from 0° to 360°. Finally, several measurements should be made with the control voltages set for nearly maximum attenuation. This allows one to verify the correctness of the model by its ability to predict behavior near null (maximum attenuation).

To obtain an initial estimate of γ and τ_1 we can solve equations 16 and 17 for γ and τ_1 given values for S_a and S_p estimated from measured data for a particular A and ϕ. (The γ and τ_1 values determined in this way would be the exact answer if the model were perfect and the measurements noiseless.) This process can be repeated for each measured S_a, S_p pair. Then the resulting γ and τ_1 values -- which hopefully will show only a small spread -- may be averaged. These average values can then be used as a starting point in a least squares fitting routine.

Now, let us suppose we have chosen S_a, S_p, A, ϕ from a selected measurement. From Equations 16 and 17 we see that if the model holds then:

$$\frac{S_a}{S_p} = \frac{K_a}{K_p} \frac{\sin(\omega_o \tau_1 + \phi)}{\cos(\omega_o \tau_1 + \phi)} = \frac{K_a}{K_p} \tan(\omega_o \tau_1 + \phi) \tag{18}$$

which indicates that:

$$\tau_1 = \frac{1}{\omega_o} (\tan^{-1} \frac{K_p S_a}{K_a S_p} - \phi) \tag{19}$$

Having obtained τ_1 we can easily use either Equation 16 or 17 to obtain γ.

Having done this for several cases of S_a, S_p, A, and ϕ, we may wish to find the γ and τ_1 values which give the best least-squares fit to all of these several cases. This is the method by which the parameters given in the next section of this report were determined.

C. Determination of Least Squares Fit

A least squares fit is obtained by picking γ and τ_1 values which minimize a criterion of goodness. Adequate results were obtained using the criterion:

$$E = \sum_{\substack{\text{8 selected} \\ \text{measurements}}} \left[(S_a^p - S_a^m)^2/(S_a^m)^2 + (S_p^p - S_p^m)^2/(S_p^m)^2 \right] \qquad (20)$$

where S_a^p, S_p^p denote the predictions which the model makes for S_a and S_p when given a value of γ and of τ_1, and S_a^m, S_p^m denote the measured values. It should be recognized that S_a^m and S_p^m are functions of A and ϕ, that S_a^p and S_p^p are functions of γ, τ_1, A, and ϕ (see equations 16 and 17), and that the summation in Equation 20 is over a set of A and ϕ values.

A strategy for picking γ and τ_1 to minimize E is to allow γ to vary over a reasonable range in a computer program loop and manually enter successive values of τ_1 to minimize E. Each run of the program uses a single τ_1 value and tries each γ value in the loop to find which one minimizes E. The program then prints out the γ value which minimized E for the given τ_1 value and what value of E resulted. The user then picks another value of τ_1 and reruns the program -- stopping when E is deemed small enough. This strategy avoids the complexity of a gradient search method and was found not to take too much operator time.

IV. MEASUREMENTS

Extensive measurements of the frequency response of transconductance multiplier weight circuits #2 and #3 were made on a Hewlett-Packard network analyzer. Values of γ, τ_1, and τ_2 were determined as described above and then plugged into a program which simulated the entire model shown in Figure 5. In both weight circuits very good agreement between model and measurement was obtained (see Figures 7-16).

The values of γ, τ_1, and τ_2 determined were as follows:

WEIGHT #2	WEIGHT #3

$\gamma = 7.86 \times 10^{-4}$ $\gamma = -6.52 \times 10^{-4}$

$\tau_1 = 4.66$ nanoseconds $\tau_1 = 4.15$ nanoseconds

$\tau_2 = 5.7$ nanoseconds $\tau_2 = 5.7$ nanoseconds

Although the gains of the I and Q paths were not precisely equal, they were never more than about 1 dB apart so it is reasonable to speak of a single insertion loss figure of between 12 and 13 dB for both weight circuits #2 and #3. It should be emphasized that in these plots (as well as in the rest of this report) all attenuation values are the actual attenuation that the circuit produces. There has been no correction for average insertion loss, overall time delay, or any other effects.

A number of plots were made of measured and predicted frequency response. See for example Figures 7 through 16. Solid lines are the measured data and dotted lines are the data predicted by the model. Perhaps the most striking feature of these plots is that even though all the curve fitting was done with straight line data (as shown in Figures 9, 10, 15, 16) the model still manages to predict the measured data even when this data is very curved (as shown in Figures 7, 8, 11, 12, 14). The data is for weight circuit #3.

V. CONCLUSIONS

As inspection of Figures 7 through 16 will indicate, it is possible to obtain a simple model of the transconductance multiplier weight circuit with parameters determined from measured data on individual circuits. This model allows prediction of antenna nulling system performance and thus allows one to intelligently specify the performance requirements on the weight circuits needed to achieve a specified degree of interference cancellation or conversely to infer from the state-of-the-art in multiplier circuits the amount of interference cancellation achievable with antenna nulling systems due to multiplier limitations.

REPORT DOCUMENTATION PAGE	READ INSTRUCTIONS BEFORE COMPLETING FORM

1. REPORT NUMBER	2. GOVT ACCESSION NO.	3. RECIPIENT'S CATALOG NUMBER
ESD-TR-79-161		

4. TITLE *(and Subtitle)*	5. TYPE OF REPORT & PERIOD COVERED
Characterization of Transconductance Multiplier Weight Circuits for an Adaptive Antenna System	Technical Note
	6. PERFORMING ORG. REPORT NUMBER
	Technical Note 1979-23

7. AUTHOR(s)	8. CONTRACT OR GRANT NUMBER(s)
Bruce C. Levens	F19628-78-C-0002

9. PERFORMING ORGANIZATION NAME AND ADDRESS	10. PROGRAM ELEMENT, PROJECT, TASK AREA & WORK UNIT NUMBERS
Lincoln Laboratory, M.I.T. P.O. Box 73 Lexington, MA 02173	Program Element No. 63431F Project No. 1227

11. CONTROLLING OFFICE NAME AND ADDRESS	12. REPORT DATE
Air Force Systems Command, USAF Andrews AFB Washington, DC 20331	22 June 1979
	13. NUMBER OF PAGES
	34

14. MONITORING AGENCY NAME & ADDRESS *(if different from Controlling Office)*	15. SECURITY CLASS. *(of this report)*
Electronic Systems Division Hanscom AFB Bedford, MA 01731	Unclassified
	15a. DECLASSIFICATION DOWNGRADING SCHEDULE

16. DISTRIBUTION STATEMENT *(of this Report)*

Approved for public release; distribution unlimited.

TN-1979-23

17. DISTRIBUTION STATEMENT *(of the abstract entered in Block 20, if different from Report)*

18. SUPPLEMENTARY NOTES

None

19. KEY WORDS *(Continue on reverse side if necessary and identify by block number)*

space communications	multiplier weight circuits
interference cancellation	adaptive antenna
transconductance	antenna nulling

20. ABSTRACT *(Continue on reverse side if necessary and identify by block number)*

Extensive testing of the transconductance multiplier weight circuits designed for the antenna nulling project indicates that a simple time delay feedthrough model fits the measured data very well. Properties of this model are derived and applied to the problem of determining the model parameters from measured data. Plots of actual measurements and model predictions are provided to demonstrate goodness of fit.

DD FORM 1473 1 JAN 73   EDITION OF 1 NOV 65 IS OBSOLETE